





# Annual Yield Simulation of Solar Parks With SubMPPT

Sascha Eckerter<sup>1,\*</sup> , Patrick Mader<sup>1</sup> , Sebastian Coenen<sup>1</sup> , and Rainer Merz<sup>1</sup> 

<sup>1</sup>University of Applied Science Karlsruhe, Germany

\*Correspondence: Sascha Eckerter, [sascha.eckerter@h-ka.de](mailto:sascha.eckerter@h-ka.de)

**Abstract.** Solar power generation plays a crucial role in the energy transition, especially in countries like Germany where the area for photovoltaic power plants is limited. This study uses simulations to show how Substring Maximum Power Point Tracking technology improves the space utilization rate of photovoltaic power plants compared to conventional String Maximum Power Point Tracking and bypass diodes. The simulation uses the Python library Pvlb and a single-diode model to calculate the current-voltage characteristics of each substring within the solar modules. When the spacing between module rows decreases, the number of modules per area increases, but so does partial shading. In conventional systems, this shading leads to higher energy losses. Substring Maximum Power Point Tracking actively reduces these losses by regulating each substring individually. Substring Maximum Power Point Tracking reduces these losses, resulting in a +10.03 % increase in space utilization rate and a +22.22 % increase in annual energy yield compared to String Maximum Power Point Tracking when the row spacing is minimized. With larger row spacing and less shading, the advantage of Substring Maximum Power Point Tracking is lower, even leading to a –2.76 % decrease in space utilization rate. The simulations confirm that selecting the optimal row spacing is essential for maximizing economic efficiency. Future research will include an economic assessment of different solar park designs using Substring Maximum Power Point Tracking.

**Keywords:** Annual Energy Yield Simulation, SubMPPT, Space Utilization Rate, Pvlb

## 1. Introduction

The growth of solar energy generation plays an important role in the energy transition. In nations such as Germany, the space available for photovoltaic (PV) installations is restricted. Minimizing row spacing enhances the potential installed PV capacity within a given area. This leads to increased row shading within the solar park, depending on the position of the sun [1]. Space utilization rate (SUR), also known as land use efficiency, quantifies the efficiency of PV installations by measuring the energy output generated per area. Current technologies such as String Maximum Power Point Tracking (StringMPPT) and bypass diodes, result in energy yield losses during partial row shading as a consequence of the series connection of the substrings and modules [2]. Therefore, the reduction of row spacing is limited, as it represents a compromise between installed power and energy losses. Currently, researchers simulate solar systems with module optimization technology using buck converters to study shading losses at the module level more accurately [3]. Technologies like Substring Maximum Power Point Tracking (SubMPPT) can increase the SUR of PV power plants by mitigating the impact of partial shading at the substring level [4, 5, 6]. The energy conversion efficiency of SubMPPT is not 100% due to non-ideal components. The three buck converters that comprise the SubMPPT technology cause electronic circuit losses depending on the currents and voltages of the respective substrings [7]. Currently, there is no simulation to determine these circuit

losses and the annual energy yield of PV parks with SubMPPT. This study analyzes the SUR with StringMPPT and SubMPPT, including electronic losses, and compares the simulation results. The irradiation at substring level is the input for the power and yield simulations of solar parks with StringMPPT and SubMPPT [1]. The Python library Pvlb calculates the electrical characteristics of the substrings using the single-diode model [8]. Chapter 0 explains the simulation of the current-voltage ( $IV$ ) characteristics of StringMPPT in more detail. Chapter 0 explains how the SubMPPT circuit works and describes the simulation of SubMPPT. Chapter 0 describes the solar parks examined in this work and determines the SUR of the facilities. Chapter 0 and Chapter 0 present and evaluate the simulation results.

## 2. Simulation StringMPPT

The simulation of StringMPPT combines the  $IV$  characteristics of all substrings within a PV string into an overall string  $IV$  characteristic. Connecting the bypass diodes parallel to the substrings ensures efficient operation and protection against voltage fluctuations. This simulation also incorporates the forward voltage of the bypass diodes.

**Figure 1** shows a simulation of a string inverter with StringMPPT in the morning with edge shading effects. A string includes 21 modules with an open circuit voltage  $V_{OC,M} = 47.6 V$  and a short circuit current  $I_{SC,M} = 11.3 A$  of each module. Each module includes three substrings with an open circuit voltage  $V_{OC,S} = 15.86 V$ . The Schottky bypass diodes sb3050dy have a forward voltage  $V_F = 0.55 V$ . The previously simulated tilted global irradiation values at substring level of the upper substrings  $G_{T1} \approx 389 W/m^2$ , the middle substrings  $G_{T2} \approx 186 W/m^2$  and the lower substrings  $G_{T3} \approx 71 W/m^2$  with constant direct irradiation as well as the global tilted irradiation of the edge shaded substrings serve as input values. The simulation of the irradiation data considers inhomogeneities of diffuse shading and edge effects [1]. The Python library Pvlb calculates the  $IV$  characteristics of each substring based on the irradiation data and module parameters using the single-diode model. All  $IV$  characteristics of the substrings within a PV string are combined into one string  $IV$  characteristic with string current  $I_S$  and string voltage  $V_S$ . The  $IV$ -characteristic progression at approximately  $V_S = 310 V$  and  $V_S = 650 V$  demonstrates the simulated forward of the bypass diodes of edge shaded substrings. With the String  $IV$  characteristic the simulation program calculates the MPP of the String. This considers the effects of shading, the forward voltage of the bypass diodes and the efficiency of the power conversion of the inverter.

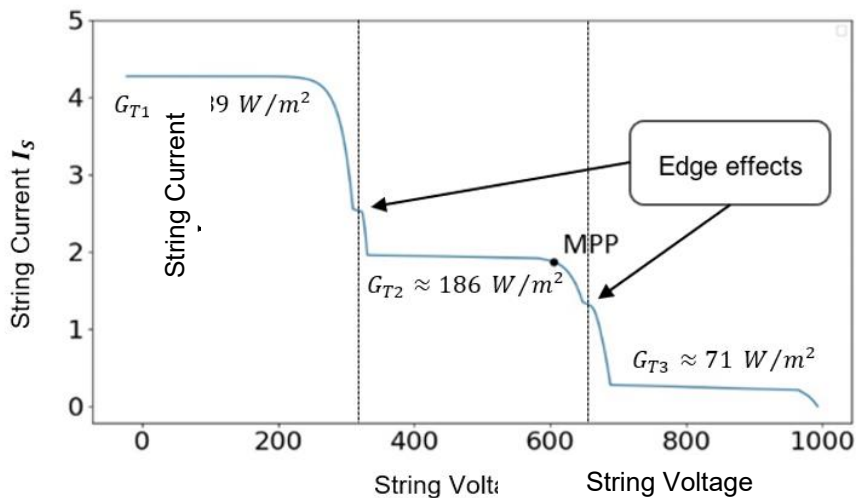


**Figure 1.** Simulation of  $IV$  characteristic of a PV string with StringMPPT, forward voltage  $V_F = 0.55 V$  of the bypass diodes and edge shading effects at  $V_S = 310 V$  and  $V_S = 650 V$ .

### 3. Simulation SubMPPT

The SubMPPT simulation uses a detailed methodology to calculate the power output of the PV park with SubMPPT. The model code takes into account the specific operating characteristics and associates them with the efficiency of a buck converter for power conversion,  $\eta_b < 100\%$  [9, 10]. The irradiation data of each substring of all modules in the simulated solar park are the input parameters for the  $IV$  characteristic simulation with SubMPPT. Pvlb functions simulate the  $IV$  characteristics for each substring within a module using the single-diode model.

**Figure 2** shows the block diagram of the SubMPPT with a connected PV-Module and its substrings S1, S2, and S3. Each module consists of three bypass diodes, one for each substring. Each SubMPPT has three MPPTs, with one connected to each substring. The MPPTs are connected in a single circuit and configured as step-down converters [7]. The SubMPPT comprises a voltage balancer with DC-DC converters X1 and X2 and Current adjustment with X3. The SubMPPT adjusts the three substring voltages  $V_1$ ,  $V_2$  and  $V_3$  so that each substring operates at its MPP. The currents of the substrings  $I_1$ ,  $I_2$  and  $I_3$  determine the output currents of the converters  $I_{L1}$ ,  $I_{L2}$  and  $I_{out}$ . Kirchhoff's current law and the duty circles  $d_1$  and  $d_2$  of X1 and X2 describe the node equations, which express the functional dependencies of  $I_{L1}$ ,  $I_{L2}$  and  $I_{out} = 1/d_3 \cdot i_0$  with  $i_0 = i_1 + i_{D1} - d_1 i_{L1} - d_2 i_{L2}$ . The input voltages  $V_1$  and  $V_2$  of converters X1 and X2, as well as the input voltage  $V_0$  of converter X3, define the electronic circuit losses together with the output currents  $I_{L1}$ ,  $I_{L2}$  and  $I_{out}$ .

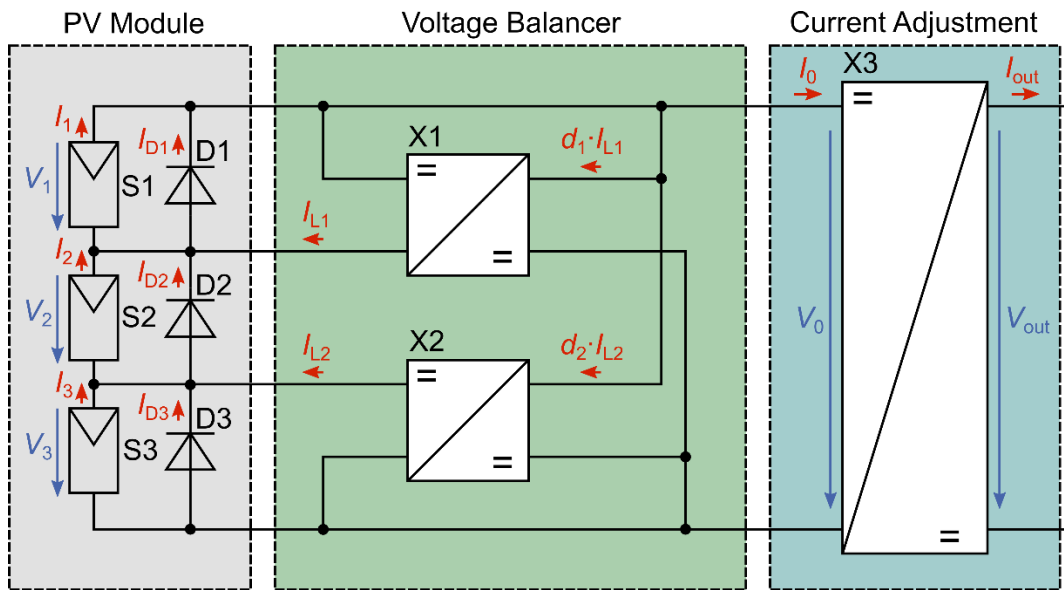


**Figure 2.** Block diagram of the SubMPPT with the connected PV module and its substrings S1, S2, and S3. The SubMPPT consists of the voltage balancer with the DC-DC converters X1 and X2 and the current adjustment with X3.

The MPP-Voltage  $V_{n,mpp}$  and the MPP-Current  $I_{n,mpp}$  of the substrings  $S_n$  with  $n = 1,2,3$  describe the power output  $P_{out} = i_{out} \cdot V_{out}$  of a module with SubMPPT including the losses of the Voltage Balancer and the Current Adjustment.

### 4. Simulation of Solar Parks

The most common scenario at the beginning of solar park planning is that a certain area is available, and it should be filled with the maximum possible number of solar modules. Among other factors, row-to-row shading effects limit the number of installable module rows and thus the SUR of the solar park. This chapter shows three different solar parks with varying numbers

of module rows. The further simulation of these solar parks with StringMPPT and SubMPPT investigates whether SubMPPT increases the SUR. Row-to-row shading reduces the current because even a small shadow on one cell sets the current for every series-connected cell within the same substring. When installers mount modules in portrait orientation, a horizontal shadow from the next row strikes all vertical substrings and throttles the entire module. By contrast, landscape orientation confines the same shadow to the lower, horizontally aligned substrings. SubMPPT then tracks only these shaded substrings and keeps the rest of the module at its optimum operating point. Thus, module orientation directly governs both the magnitude of shade-induced current mismatch and the effectiveness of SubMPPT.

**Figure 3** illustrates the three south-facing solar park variants SP1, SP2, and SP3 with landscape oriented  $370\text{ Wp}$  modules for the simulation of StringMPPT and SubMPPT. The modules have a length  $L = 1.13\text{ m}$  and a width  $B = 1.87\text{ m}$ , and the tilt is  $\beta = 30^\circ$ . The area of all three parks is  $A = 400.0\text{ m}^2$ . The solar parks consist of  $21 \times 1$  solar module arrays per row. The specified number of module rows determines the arrangement. The optimal row spacing  $D$  between the top edges of the module rows maximizes the utilization of the available area. Figure 3 a) shows solar park SP1 with a row spacing  $D = 1.84\text{ m}$  and six module rows. Figure 3 b) depicts solar park SP2 with a reduced row spacing of  $D = 1.32\text{ m}$  and eight module rows. Figure 3 c) shows solar park SP3 with ten module rows and  $D = 1.02\text{ m}$ . Compared to SP1, SP2 has +25 %, and SP3 +40 % more modules installed.

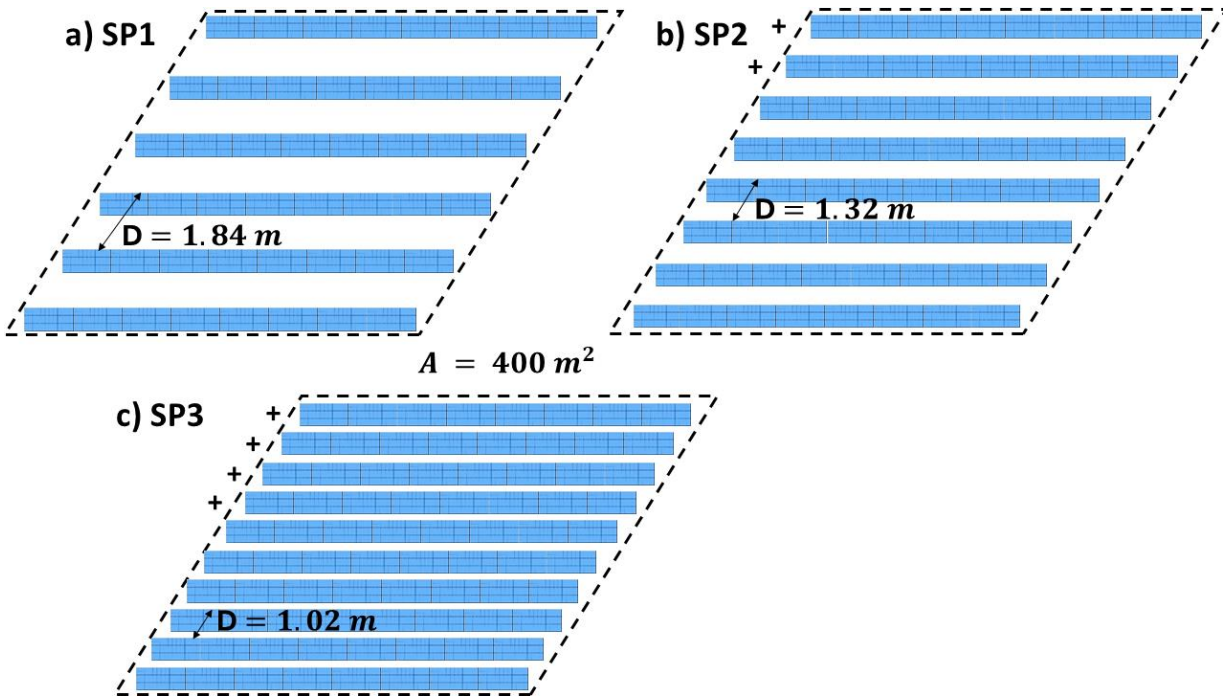


**Figure 3.** The Solar Park Areas  $A = 400.0\text{ m}^2$  are oriented south and the modules tilt is  $\beta = 30^\circ$ .

- a) Solar park SP1 with a row spacing  $D = 1.84\text{ m}$  and six module rows.
- b) Solar park SP2 with a reduced row spacing of  $D = 1.32\text{ m}$  and eight module rows.
- c) Solar park SP3 with ten module rows and  $D = 1.02\text{ m}$ .

## 5. Results

**Figure 4** describes the simulated monthly energy yield  $E_M$  of SP1, SP2, and SP3. The relative difference  $\delta_n = (E_{M,Sub,n} - E_{M,Str,n})/E_{M,Sub,n}$  with  $n = 1,2,3$  describes the difference between the monthly energy yield  $E_M$  with SubMPPT compared to StringMPPT. In solar park SP1, there is hardly any direct shading during the year, and the inhomogeneity of diffuse irradiation is small compared to narrower row spacing  $D$  as in SP2 or SP3. Due to the electronic circuit losses of SubMPPT, StringMPPT is more efficient than SubMPPT for the whole year but

February. The simulation of solar park SP2 reduces the row spacing to  $D = 1.32 \text{ m}$ . The reduced row spacing increases both the direct row-to-row shading and the inhomogeneous diffuse irradiation. In the winter months from November to February, the solar zenith in the Northern Hemisphere is lower than in the summer months from May to August. Therefore, the system of SP2 equipped with SubMPPT converts more solar irradiation into electrical energy than that with StringMPPT in winter. In summer from May to August there is less partial shading and so StringMPPT is more efficient than SubMPPT. Solar park SP3 shows a similar trend with even more reduced row spacing of  $D = 1.02 \text{ m}$ . The simulation of SP3 depicts that SubMPPT is more efficient than StringMPPT, when partial shading occurs all over the year.

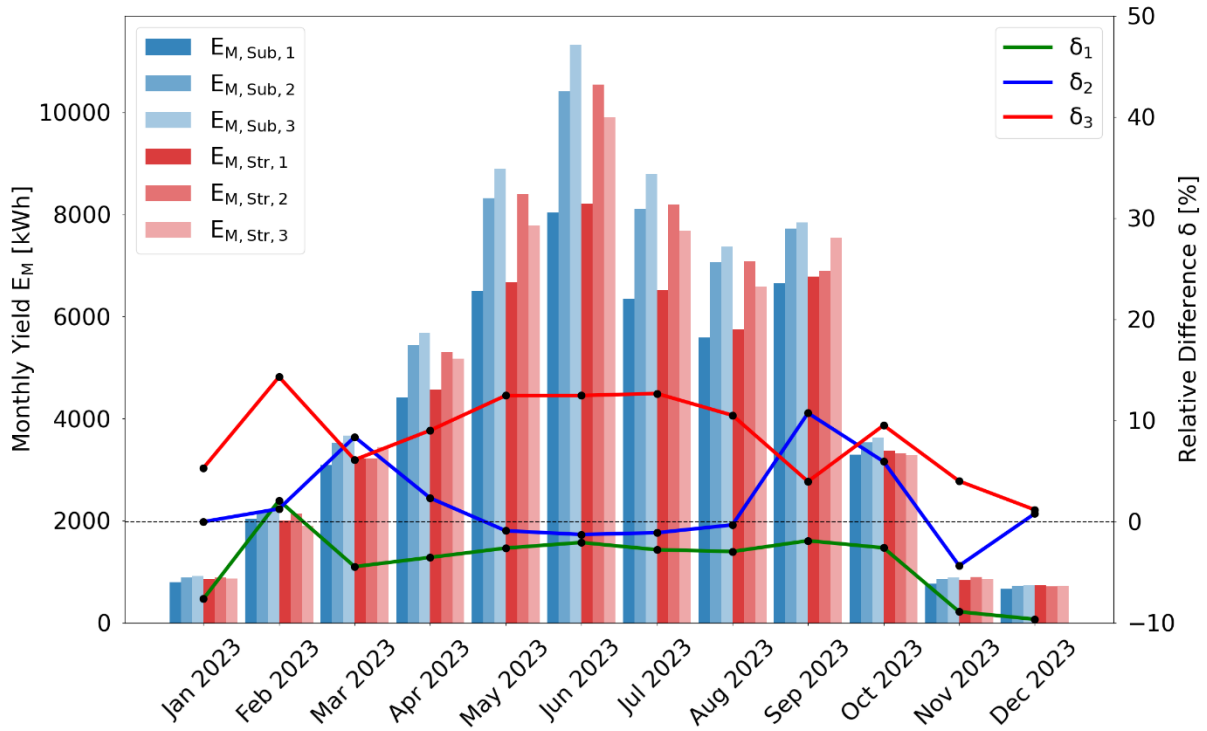


**Figure 4.** Simulation of the monthly energy yield  $E_M$  of the solar parks SP1, SP2, and SP3 with SubMPPT and StringMPPT and the relative difference  $\delta_n$ .

**Figure 5** shows the annual energy yield  $E_Y$  of the simulation of solar parks SP1, SP2, and SP3 with SubMPPT and StringMPPT and their relative difference  $\delta_{E,n}$ . There is almost no partial shading in SP1 because row shading hardly occurs due to the large row spacing  $D$ . The annual total energy yield of SP1 with the SubMPPT system is  $E_{Y,Sub,1} = 48\,197 \text{ kWh}$  and with the String-MPPT system  $E_{Y,Str,1} = 49\,527 \text{ kWh}$ . The annual relative energy yield difference of SP1  $\delta_{E,1} = (E_{Y,Sub,1} - E_{Y,Str,1})/E_{Y,Sub,1} = -2.76 \%$  indicates that the SubMPPT technology achieves a lower energy yield compared to the StringMPPT technology when nearly no partial shading occurs. The total annual energy yield of SP2 of the SubMPPT system is  $E_{Y,Sub,2} = 58\,770 \text{ kWh}$  and that of the String-MPPT system  $E_{Y,Str,2} = 57\,630 \text{ kWh}$ . The relative annual energy yield difference of SP2 is  $\delta_{E,2} = 1.94 \%$ . Due to more installed module rows but also more row-to-row shading, the total annual energy yield  $E_{Y,2} > E_{Y,1}$ . Compared to the first two solar parks SP1 and SP2, the annual energy yield of SP3 with SubMPPT is  $E_{Y,Sub,3} = 61\,969 \text{ kWh}$  and with StringMPPT  $E_{Y,Str,3} = 55\,752 \text{ kWh}$ . The relative annual energy yield difference of SP3 is  $\delta_{E,3} = 10.03 \%$ . This means that SubMPPT achieves significantly more energy yield at minimal row spacing compared to StringMPPT. The comparison of the absolute energy yield corresponds to  $E_{Y,Sub,3} = 122 \% \cdot E_{Y,Sub,1}$ , resulting in a higher energy yield with SubMPPT of SP3 compared to the configuration of SP1. In contrast, StringMPPT achieves  $E_{Y,Str,3} = 111 \% \cdot E_{Y,Str,1}$  more energy yield when comparing SP3 to SP1. The comparison of the solar parks SP1, SP2, and SP3 thus shows that modules fitted



with bypass diodes reach their highest energy yield at the intermediate row spacing defined by configuration SP2. Energy output drops when the spacing increases to SP1 or decreases to SP3. So, there is an optimal row spacing for StringMPPT. Using SubMPPT and progressively reducing row spacing always raises the energy yield.

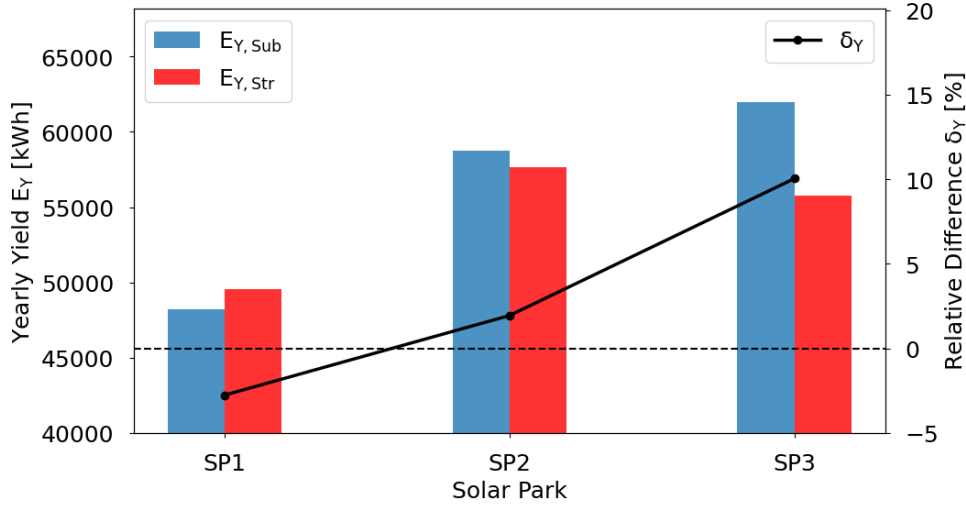


**Figure 5.** Presentation of the annual energy yields of the solar parks SP1, SP2, and SP3 with SubMPPT and StringMPPT and the relative difference  $\delta_E$ .

In conclusion the simulation also shows that +40.00% more installed modules achieve +22.22 % more electrical energy output with SubMPPT and only +11.17 % more energy output with StringMPPT.

The  $SUR = E/A$  indicates how much energy output  $E$  per area  $A$  is generated and enables a consistent comparison of solar parks with different areas.

**Figure 6** shows the monthly SUR and the average SUR per year as energy yield per area for the solar parks SP1, SP2 and SP3 with SubMPPT and StringMPPT. Solar parks SP3 and SP2 with SubMPPT achieve the highest yearly space utilization rate with  $SUR_{Y, Sub, 3} = 12.91 \text{ kWh/m}^2$  and  $SUR_{Y, Sub, 2} = 12.24 \text{ kWh/m}^2$ . The following are the solar parks with StringMPPT SP2 with  $SUR_{Y, Str, 2} = 12.01 \text{ kWh/m}^2$ , SP3 with  $SUR_{Str, 3} = 11.62 \text{ kWh/m}^2$ , and SP1 with  $SUR_{Y, Str, 1} = 10.32 \text{ kWh/m}^2$ . The lowest SUR is achieved by SP1 with SubMPPT with  $SUR_{Y, Sub, 1} = 10.04 \text{ kWh/m}^2$ . Since the area  $A = 400 \text{ m}^2$  of the solar parks SP1, SP2, and SP3 is the same, the relative differences  $\delta_{SUR, n} = (SUR_{Y, Sub, n} - SUR_{Y, Str, n}) / SUR_{Y, Sub, n} = \delta_{E, n}$  with  $n = 1, 2, 3$  are also equal to the annual relative energy yield differences.

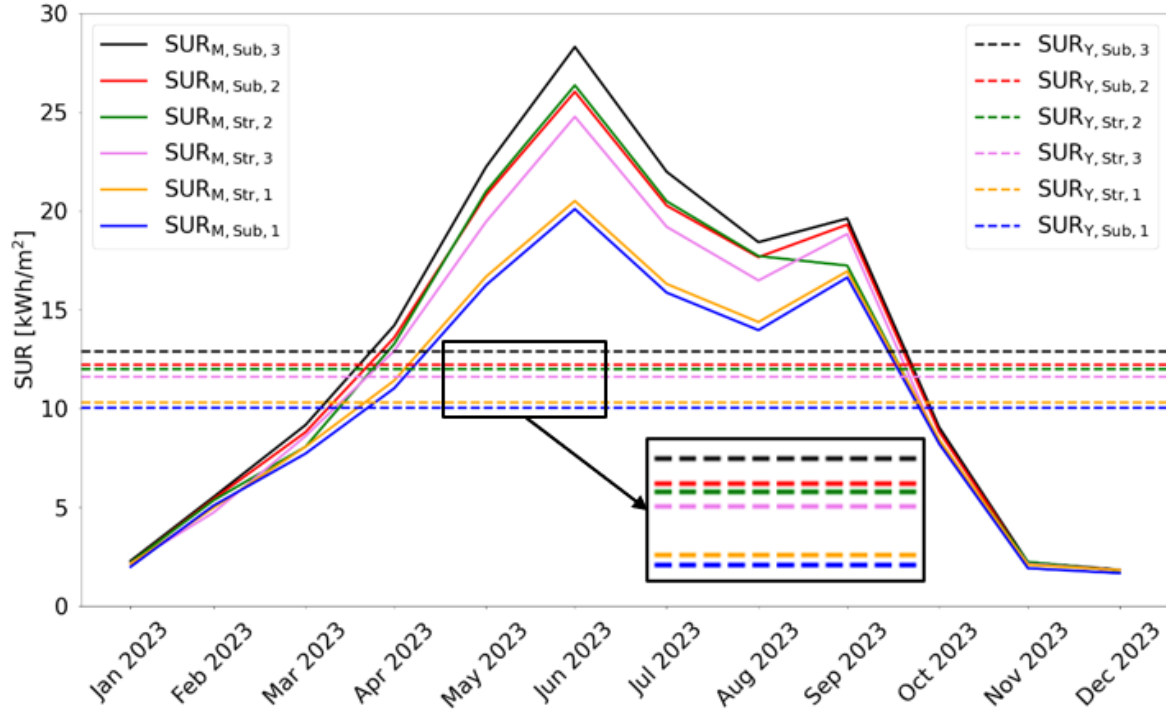


**Figure 6.** Monthly  $SUR_M$  and yearly  $SUR_Y$  space utilization rate of the solar parks SP1, SP2, and SP3.

The simulation shows that SubMPPT achieves a lower SUR than StringMPPT with a large row spacing and thus slight partial shading as in SP1. Reducing the row spacing improves the SUR of the solar park with SubMPPT compared to StringMPPT as the simulation of SP2 and SP3 shows.

## 6. Conclusion

An optimal Space Utilization Rate of a photovoltaic park is important to maximize the annual energy yield of a given area. With SubMPPT, it is possible to gain more energy yield through electronic circuits instead of solely focusing on increasing the modules' efficiency. Simulations of various solar parks demonstrate that SubMPPT increases the Space Utilization Rate depending on the degree of partial shading. The simulated parks in this paper have the same area but vary in row spacing of the modules, the number of installed modules, and whether StringMPPT or SubMPPT technology is integrated. A larger row spacing reduces the number of modules installed and consequently decreases the energy output per area. Conversely, a smaller row spacing increases partial shading, which in turn reduces energy output per installed power. Selecting a row spacing large enough to minimize row-to-row shading, the SubMPPT is not able to gain energy and the limited efficiency of SubMPPT results in a worse Space Utilization Rate for SubMPPT of  $-2.76\%$ . Reducing the row spacing in order to maximize the number of modules, the SUR of the solar park with SubMPPT compared to StringMPPT raises to up to  $+10.03\%$ . The simulation also shows that  $+40\%$  more installed modules achieve  $+22.22\%$  more electrical energy output with SubMPPT and only  $+11.17\%$  more energy output with StringMPPT.

The results suggest that for an economic analysis of PV parks with SubMPPT, there exists an optimal row spacing for maximizing return on investment. Considering actual module prices and their small percentage to the total cost of solar parks, it is conceivable to accept partial shading and reduce the row spacing to install more module rows on the available area. Parks with SubMPPT then achieve a significantly higher SUR than parks with StringMPPT. The next

step involves an economic simulation of the costs of PV parks with SubMPPT to determine the most cost-effective row spacing.

## Data availability statement

The authors do not have permission to share data.

## Author contributions

Conceptualization, S.E., P.M., S.C., R.M.; Methodology, S.E.; Software, S.E.; Validation, S.E., P.M., R.M.; Formal Analysis, S.E., S.C., R.M.; Investigation, S.E.; Resources, S.E., R.M.; Data Curation, S.E.; Writing – Original Draft Preparation, S.E.; Writing – Review & Editing, S.E., S.C., R.M.; Visualization, S.E.; Supervision, S.E., P.M.; Project Administration, S.E., R.M.; Funding Acquisition, R.M.

## Competing interests

The authors declare that they have no competing interests.

## Funding

This work contributes to the research performed at the University of Applied Science Karlsruhe. The results were generated within the project "Solarpark 2.0" (funding code 03EE1135C) funded by the Federal Ministry for Economic Affairs and Climate Action (BMWK).

## Acknowledgement

The authors thank the Federal Ministry for Economic Affairs and Climate Action and the project management organization Julich (PTJ) for funding this work.

## References

- [1] S. Eckerter, K. Kerekes, P. Mader und R. Merz, „Analysis of Irradiation Differences on Substringlevel in Solar Parks,“ 41th EUPVSEC, 2024.
- [2] I. Mehedi, Z. Salam, M. Ramli, V. Chin, H. Bassi, M. Rawa und M. Abdullah, „Critical evaluation and review of partial shading mitigation methods for grid-connected PV system using hardware solutions: The module-level and array-level approaches,“ Renewable and Sustainable Energy Reviews, Bd. 146, pp. 111-138, 2021.
- [3] C. Allenspach, F. Carigiet, A. Bänziger, A. Schneider und F. Baumgartner, „Power Conditioner Efficiencies and Annual Performance Analyses with Partially Shaded Photovoltaic Generators Using Indoor Measurements and Shading Simulations,“ RRL Solar, 2023.
- [4] S. Enkhardt, „pv-magazin.de,“ pv magazin, 30 06 2024. [Online]. Available: <https://www.pv-magazine.de/2022/10/19/projekt-solarpark-2-0-mehr-photovoltaik-leistung-auf-der-gleichen-flaeche/>. [Zugriff am 19 10 2022].
- [5] R. Brace, A. Neumann, T. Czarnecki und R. Merz, „Substring-MPPT for 4-Terminal 3-Substring Modules,“ in EU PVSEC 2018, 2018.
- [6] R. Merz, S. Eckerter, S. Coenen und P. Mader, „Substring-MPPT steigert Strangleistung bei Teilverschattung,“ In Tagungsunterlagen 39. PV-Symposium , 2024.
- [7] P. Mader, S. Eckerter und R. Merz, „DESIGN OF THE SUBSTRING MPP TRACKER,“ 41th EUPVSEC, 2024.



- [8] K. Anderson, C. Hansen, W. Holmgren, A. Jensen, M. Mikofski und A. Driesse, „pvlib python: 2023 project update,“ *Journal of Open Source Software*, Bd. 8(92), Nr. 5994, 2023.
- [9] G. Lakkas, „MOSFET power losses and how they affect power-supply efficiency,“ *Analog Applications Journal*, pp. 22-26, 2016.
- [10] Rohm Semiconductor, „Efficiency of Buck Converter,“ ROHM Co., Ltd., 2022.